



Provided by the author(s) and University of Galway in accordance with publisher policies. Please cite the published version when available.

Title	Salts, binary and ternary cocrystals of pyrimethamine: mechanosynthesis, solution crystallization and crystallization from the gas phase
Author(s)	O'Malley, Ciaran; Bouchet, Chloe; Manyara, Grayce; Walsh, Niamh; McArdle, Patrick; Erxleben, Andrea
Publication Date	2020-11-24
Publication Information	O'Malley, Ciaran, Bouchet, Chloe, Manyara, Grayce, Walsh, Niamh, McArdle, Patrick, & Erxleben, Andrea. (2020). Salts, Binary and Ternary Cocrystals of Pyrimethamine: Mechanosynthesis, Solution Crystallization, and Crystallization from the Gas Phase. <i>Crystal Growth & Design</i> . doi:10.1021/acs.cgd.0c01147
Publisher	American Chemical Society
Link to publisher's version	https://dx.doi.org/10.1021/acs.cgd.0c01147
Item record	http://hdl.handle.net/10379/16407
DOI	http://dx.doi.org/10.1021/acs.cgd.0c01147

Downloaded 2024-04-26T07:57:39Z

Some rights reserved. For more information, please see the item record link above.



Salts, Binary and Ternary Cocrystals of Pyrimethamine: Mechanosynthesis, Solution Crystallization and Crystallization from the Gas Phase

Ciaran O'Malley,¹ Chloe Bouchet,^{1,2} Grayce Manyara,¹ Niamh Walsh,¹ Patrick McArdle,^{1,*} and Andrea Erxleben^{1,3,*}

¹ School of Chemistry, National University of Ireland, Galway, H91TK33, Ireland

² ITECH Lyon, 87 chemin des Mouilles, 69134 Ecully Cedex

³ Synthesis and Solid State Pharmaceutical Centre (SSPC), Limerick, V94T9PX, Ireland

*Corresponding author email address: andrea.erxleben@nuigalway.ie (AE);

p.mcardle@nuigalway.ie (PM)

Abstract

A series of salts and binary and ternary cocrystals of the antimalaria drug pyrimethamine (PYR) are reported. PYR has a donor-acceptor-donor (DAD) and a donor-acceptor (DA) binding site and cocrystallization experiments were carried out with coformers with complementary ADA and AD H bonding functionalities. Three different preparation techniques were compared; solution crystallization, crystallization from the gas phase and liquid-assisted grinding. In several cases different solid-state forms were obtained depending on the crystallization method. The molecular ionic cocrystals $\text{PYRH}^+\text{BAR}^-\cdot\text{PYR}$ (BAR = barbituric acid) and $(\text{PYRH}^+\text{SAC}^-)_2\cdot\text{GLU}$ (GLU = glutarimide, SAC = saccharin), the binary cocrystal $\text{PYR}\cdot\text{GLU}$, the salt $\text{PYRH}^+\text{NIC}^-$ (NIC = nicotinic acid) and two polymorphs of $\text{PYRH}^+\text{SAC}^-$ could be crystallized by sublimation. Two other ternary molecular ionic cocrystals, $(\text{PYRH}^+\text{BEN}^-)\cdot\text{PYR}\cdot\text{SUC}$ and $(\text{PYRH}^+\text{SAC}^-)_2\cdot\text{SOR}$ (SUC = succinimide, BEN = benzoic acid, SOR = sorbic acid) were obtained by solution crystallization. Attempts to crystallize ternary cocrystals from solution also yielded a number of new two-component cocrystals including four new solvates of $\text{PYRH}^+\text{SAC}^-$, thus extending the structural landscape of the PYR/SAC system. Liquid-assisted milling was carried out as a one-pot reaction and with the stepwise addition of the coformers. The $(\text{PYRH}^+\text{SAC}^-)_2\cdot\text{GLU}$ cocrystal formed when the coformers were milled in one step and when

they were added to the mill stepwise. For other systems the outcome of the two-step milling experiment depended on the order in which the cofomers were added. The PYR-coformer interactions were analyzed using the PIXEL programme.

INTRODUCTION

The various functional groups that mediate drug-target recognition make drug molecules interesting candidates for crystal engineering. Pharmaceutical cocrystals are multi-component crystalline solids, containing two different drugs or one drug and an inactive cofomer, held together through supramolecular interactions.¹ Molecular ionic cocrystals have recently been defined as solids that are formed by cocrystallization of organic compounds that are all solids under ambient conditions, that contain charge-assisted hydrogen bonds as a result of one or more proton transfer events and that can be of type A^-BH^+AH or A^-BH^+CH .² The design and synthesis of cocrystals containing more than two components is significantly more challenging than the assembly of two cofomers, but can further enhance the functionality and performance of supramolecular materials. Although ternary cocrystals are becoming more abundant, their number is still small compared to the more numerous two-component systems.³⁻²¹ The isolation of ternary cocrystals is not trivial, as there is always the risk that a binary cocrystal will crystallize instead. Aakeröy and coworkers were the first to use a central linking molecule (isonicotinamide) that selectively hydrogen bonds to two cofomers (3,5-dinitrobenzoic acid and a substituted benzoic acid that is a weaker acid than 3,5-dinitrobenzoic acid).⁴ In line with Etter's rules,²² 3,5-dinitrobenzoic acid as the stronger acid and thus the better H bond donor interacts with the pyridine nitrogen of isonicotinamide as the best acceptor, while the weaker acid forms an $R_2^2(8)$ H bonding motif with the weaker amide acceptor. Other design strategies for the generation of ternary cocrystals include the incorporation of another cofomer into voids in the crystal lattice of a two-component cocrystal²⁰ and the replacement of the weaker synthon in a binary cocrystal with a molecule of similar size and shape.¹¹ Alternatively to exploiting the hierarchy of supramolecular synthons^{3-5,8,21} complementary types of intermolecular interactions are used to create multi-component cocrystals. Seaton *et al.* reported ternary cocrystals in which two components are held together by H bonds while the third component binds to the dimer via a charge-transfer interaction.¹⁹ Desiraju and coworkers^{6,14} and Rissanen and coworkers^{7,16}

combined hydrogen bonding and halogen bonding. A few quaternary and quinary cocrystals as well as six-component solids have also been reported.²³⁻²⁵

Pyrimethamine (PYR, Figure 1) is a folic acid antagonist and is used to treat malaria and toxoplasmosis. Various binary cocrystals and salts of PYR with carboxylic acids,²⁶⁻³⁷ saccharin,³⁸ and sulfonates^{39,40} have been described. The most basic site is the N1 nitrogen ($pK_a = 6.94$) and $R_2^2(8)$ rings with H bonding between carboxylate and the N1-H⁺/C2-NH₂ site are a recurrent motif in PYR/carboxylic acid binary systems.²⁶⁻³⁷ Likewise, in the methanol solvated saccharin salt, the saccharin anion forms a pair of N⁻⋯H⁺N1 and C=O⋯H₂N-C2 H bonds with the N1-protonated 2-aminopyrimidine site of PYR.³⁸ Sulfa-drugs with an N(heterocycle)=CH-NH(sulfonamide) functionality have been shown to interact with the C2-NH₂/N1 site of the related 2,4-diaminopyrimidine trimethoprim, either with⁴¹⁻⁴³ or without⁴³⁻⁴⁵ proton transfer. We reasoned that from a crystal engineering viewpoint, the C2-NH₂/N3/C4-NH₂ site of PYR-carboxylates and PYR-saccharinate can be used to accommodate an additional ADA cofomer to give a ternary molecular ionic cocrystal.

Cocrystals are normally prepared by solution crystallization or mechanochemically by grinding or ball-milling. The latter does not give X-ray suitable single crystals, while solubility issues are often encountered in the former. Crystallization from the gas phase eliminates solvent effects. About two-thirds of all organic compounds are sublimable⁴⁶ and the use of a vacuum during sublimation is an additional advantage when a compound is air-sensitive. Using a small temperature gradient, slow growth rates and clean condensing area surfaces with a low level of nucleation sites can provide high quality solvent-free single crystals on a lab scale.^{47,48} Bryce and coworkers prepared X-ray suitable halogen-bonded cocrystals by placing the two cofomers at the opposite ends of a sealed glass tube in a two-zone tube furnace to control the sublimation of the two components separately.⁴⁹ Smith and coworkers⁵⁰ and our own group⁵¹ have recently shown that high quality binary cocrystals can be crystallized from the gas phase using a simpler experimental setup. We have now extended the gas phase crystallization to a ternary system.

The aim of the work described in the present paper was two-fold; (i) to design ternary molecular ionic cocrystals of PYR by binding ADA and AD cofomers to the DAD and DA binding site of PYR and (ii) to further explore the preparation of cocrystals by sublimation. Glutarimide (GLU), barbituric acid (BAR) and succinimide (SUC) were selected as ADA cofomers to hydrogen-

bond to the C2-NH₂/N3/C4-NH₂ site of PYR and nicotinic acid (NIC), benzoic acid (BEN), sorbic acid (SOR), mandelic acid (MAN) and saccharin (SAC) were chosen as AD cofomers to interact with the 2-aminopyrimidine site (Figure 1).

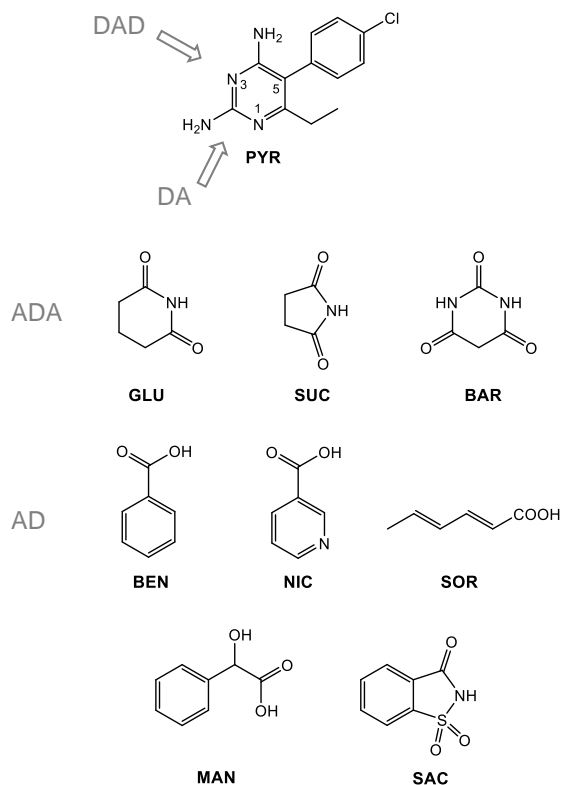


Figure 1. Chemical structures and H bond donor (D) and acceptor (A) sites of pyrimethamine and the cofomers used in this study.

EXPERIMENTAL

Materials. Pyrimethamine (PYR) and mandelic acid (MAN) were purchased from Tokyo Chemical Industry Europe. Glutarimide (GLU), succinimide (SUC), barbituric acid (BAR), saccharin (SAC), nicotinic acid (NIC), sorbic acid (SOR), and benzoic acid (BEN) were obtained from Sigma Aldrich. The solvents acetonitrile, methanol (Merck Millipore), ethyl acetate (Sigma

Aldrich), and dimethylformamide (Fisher Scientific) were analytical grade and used as received.

Ball-milling. Equimolar mixtures of PYR and the respective coformers (120 – 150 mg in total, Table S1) were placed in 2 mL Eppendorf tubes containing one 5 mm diameter stainless steel ball. 50 μ L ethanol was added to each sample. The samples were placed in an in-house 3D printed six-tube sample holder and milled at 25 Hz for 20 min. using an oscillatory ball mill (Mixer Mill MM400, Retsch GmbH & Co., Germany). In experiments where the coformers were added stepwise, the sample was milled for 20 min after each addition. The milled powder samples were analyzed immediately by X-ray powder diffraction.

Sublimation. The cocrystals and salts PYR \cdot GLU, PYRH⁺BAR⁻ \cdot PYR, PYRH⁺NIC⁻, PYRH⁺SAC⁻ I and II were crystallized from the gas phase using an in-house sublimation apparatus as previously described.⁵¹ Briefly, PYR and the respective coformer were sublimed from both ends of a standard 15 x 160 mm test tube sealed under vacuum. Two heaters were used to sublime the two components at the same rate. In the case of the ternary (PYRH⁺SAC⁻)₂ \cdot GLU cocrystal, a physical mixture of PYR and SAC was placed at one end of the test tube and GLU at the other. Two polymorphs of PYRH⁺SAC⁻ were obtained by sublimation. PYRH⁺SAC⁻ I was prepared by subliming the components as described from either end of a test tube with equalized sublimation rates. For PYRH⁺SAC⁻ II a sample of the salt was prepared by milling and sublimed at one end of the tube with a large thermal gradient used for condensation in the other end. Experimental parameters of the sublimation experiments are given in Table S2.

Solution Crystallization. 62 mg (0.25 mmol) PYR and one mole equivalent of each of the two coformers were dissolved in the minimum amount of solvent. The solvent was allowed to slowly evaporate from an open vial. Crystallization experiments were carried out in methanol, acetonitrile, ethyl acetate and dimethylformamide (Table S3). X-ray suitable single crystals of PYRH⁺NIC⁻ \cdot 1.5H₂O, PYRH⁺SAC⁻ II, PYRH⁺SAC⁻ \cdot H₂O, PYRH⁺SAC⁻ \cdot CH₃OH, (PYRH⁺SAC⁻)₂ \cdot GLU, (PYRH⁺BEN⁻) \cdot PYR \cdot SUC, (PYRH⁺SAC⁻)₂ \cdot SOR, PYRH⁺MAN⁻, and PYRH⁺SOR⁻ crystallized from methanol within a few days. PYRH⁺SAC⁻ \cdot CH₃CN crystallized from acetonitrile.

Differential Scanning Calorimetry. Differential scanning calorimetry (DSC) combined with thermogravimetric analysis was carried out in open aluminum crucibles with a STA625 thermal analyzer (RheometricScientific, Piscataway, New Jersey). The thermograms were recorded between 20 and 300°C with a heating rate of 10°C/min. Nitrogen was purged in the ambient mode. An indium standard was used for calibration.

X-ray Powder Diffraction. X-ray powder patterns were recorded on an Inel Equinox 3000 powder diffractometer (Artenay, France), fitted with a curved position sensitive detector calibrated using Y₂O₃. Cu K_α radiation ($\lambda = 1.54178 \text{ \AA}$, 35 kV, 25 mA) was used and data were collected between 5 and 90 ° (2θ). Powder patterns of the cocrystals analyzed by single crystal X-ray analysis were simulated using the Oscale software package.⁵²

Single Crystal X-ray Analysis. Single crystal X-ray diffraction was carried out on an Oxford Diffraction Xcalibur system (Oxfordshire, UK) at room temperature. The crystal structures of PYR·GLU, PYRH⁺BAR⁻·PYR, PYRH⁺NIC⁻, PYRH⁺NIC⁻·1.5H₂O, PYRH⁺SAC⁻ I, PYRH⁺SAC⁻ II, PYRH⁺SAC⁻·H₂O, PYRH⁺SAC⁻·2.2H₂O, PYRH⁺SAC⁻·CH₃OH, PYRH⁺SAC⁻·CH₃CN, (PYRH⁺SAC⁻)₂·GLU, (PYRH⁺BEN⁻)·PYR·SUC, (PYRH⁺SAC⁻)₂·SOR, PYRH⁺MAN⁻, and PYRH⁺SOR⁻ were solved by direct methods using SHELXT and refined using SHELXL 2018/3 within the Oscale package.⁵²⁻⁵⁴ Crystallographic data and details of refinement are reported in Tables 1 and S4. The cif files can be obtained free of charge at www.ccdc.cam.ac.uk/conts/retrieving.html or from the Cambridge Crystallographic Data Centre, Cambridge, UK with the REF code 2022421-2022435.

RESULTS AND DISCUSSION

Cocrystallization from the Gas Phase by Two-zone Cosublimation. To crystallize binary cocrystals from the gas phase the cofomers were placed at the opposite ends of a test tube. The test tube was sealed under vacuum and two heaters were used to sublime the cofomers at the same rate as previously described.⁵¹ X-ray suitable single crystals were obtained by cosublimation of PYR with GLU, BAR and NIC. To extend the procedure to ternary systems a third cofomer was selected that has a similar melting point to PYR. By placing a mixture of

PYR (m. p. 233 – 234 °C) and SAC (m. p. 228 °C) in one heating zone and GLU (m. p. 155 – 157 °C) in the other, the ternary cocrystal (PYRH⁺SAC⁻)₂·GLU could be successfully crystallized from the gas phase. Attempts to crystallize a ternary cocrystal of PYR with SAC and SOR from the gas phase using the same procedure gave the binary salt PYRH⁺SAC⁻ I. Single crystals of a second polymorph, PYRH⁺SAC⁻ II, were obtained, when a sample of the salt was prepared by milling (see below) and sublimed at one end of the test tube with a large thermal gradient to the other end where desublimation took place. The crystal data and hydrogen bonding interactions of (PYRH⁺SAC⁻)₂·GLU, PYR·GLU, PYRH⁺BAR⁻·PYR, PYRH⁺NIC⁻ and PYRH⁺SAC⁻ I and II are listed in Tables 1 and S5.

X-ray Structures of PYR·GLU and PYRH⁺BAR⁻·PYR. The X-ray structures of the PYR·GLU and PYRH⁺BAR⁻·PYR cocrystals are shown in Figure 2. As expected the coformers form three H bonds with the DAD site of PYR. In PYR·GLU two heterodimers assemble to create an $R_4^2(8)$ motif involving the amino protons at C4 of PYR and one carbonyl oxygen of GLU. A pair of H bonds between the 2-amino group and the N1 nitrogen of PYR generate the $R_2^2(8)$ homosynthon. In contrast to the 1:1 composition of PYR·GLU, two BAR⁻ anions (denoted BAR⁻ A and BAR⁻ B), two N1 protonated PYRH⁺ cations (denoted PYRH⁺ A and PYRH⁺ B) and two neutral PYR molecules (denoted PYR C and PYR D) make up the asymmetric unit of the molecular ionic cocrystal PYRH⁺BAR⁻·PYR. All four PYR/PYRH⁺ entities use their 2-NH₂/N3/4-NH₂ site to interact with α -carbon deprotonated BAR⁻ via NH₂···O=C/N···HN/NH₂···O=C H bonds. BAR⁻ has two C=O/N-H/C=O sites and each BAR⁻ interacts with one PYRH⁺ cation and one neutral PYR molecule (PYRH⁺ A – BAR⁻ A – PYR C and PYRH⁺ B – BAR⁻ B – PYR D). There is also H bonding between the 4-amino group of PYRH⁺ B and N1 of PYR C, between the 4-amino group of PYRH⁺ A and a carbonyl oxygen of BAR⁻ B, between the 4-amino group of PYRH⁺ B and a carbonyl oxygen of BAR⁻ B, between the 4-amino group of PYR C and a carbonyl oxygen of BAR⁻ A and between N1H⁺ of PYRH⁺ B and a carbonyl oxygen of BAR⁻ A. The N1H⁺ proton and the second C2-NH₂ proton of PYRH⁺ A form a hydrogen bond to an amide oxygen of an adjacent BAR⁻ A and to N1 of PYR D, respectively. The latter acts as a bifurcated H bond acceptor by participating in H bonding with the protonated N1 and the 2-amino group of the PYRH⁺ cation.

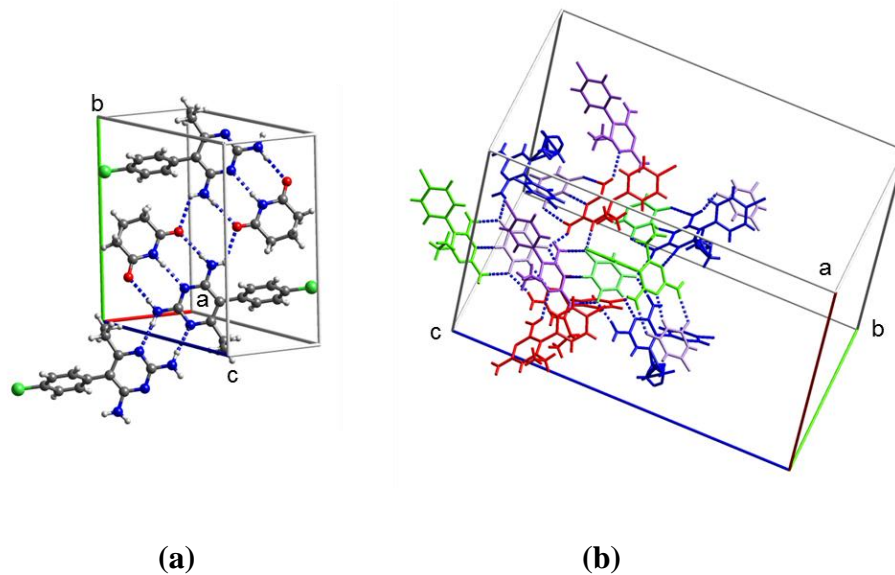


Figure 2. Hydrogen bonding motifs in the PYR·GLU (a) and PYRH⁺BAR⁻·PYR (b) cocrystals obtained by sublimation. Color code in (b): blue – PYRH⁺ A, red – PYRH⁺ B, magenta – PYR C and BAR⁻ B, green – PYR D and BAR⁻ A.

X-ray Structure of PYRH⁺NIC⁻. PYRH⁺NIC⁻ crystallizes as a salt from the gas phase. The carboxyl proton of NIC is transferred to the N1 nitrogen of PYR and the resulting PYRH⁺ cation and NIC⁻ anion interact with each other *via* the typical $R_2^2(8)$ synthon of PYR-carboxylates (Figure 3). Another $R_2^2(8)$ motif is created by a pair of N-H...N H bonds between the 4-amino group and N3 of two PYRH⁺. Two heterodimers are connected through H bonding interactions between the second proton of the amino group at C2 of PYRH⁺ and the pyridine nitrogen of NIC⁻ ($R_4^4(16)$ motif). The second amino proton at C4 is not involved in H bonding.

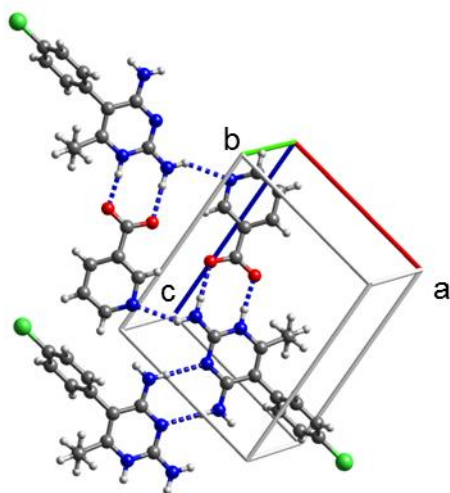


Figure 3. Hydrogen bonding motifs in the $\text{PYRH}^+\text{NIC}^-$ salt obtained by sublimation.

X-ray Structures of $\text{PYRH}^+\text{SAC}^-$ I and II. So far, only the $\text{PYRH}^+\text{SAC}^- \cdot \text{CH}_3\text{OH}$ solvate has been reported in the literature.³⁸ Figure 4 shows the X-ray structure of the unsolvated $\text{PYRH}^+\text{SAC}^-$ I salt obtained by sublimation. The structure has the usual $R_2^2(8)$ motif with $\text{N1H}^+ \cdots \text{O}=\text{C}$ and $\text{C2-NH}_2 \cdots \text{N}^-$ H bonds between PYRH^+ and SAC^- . Furthermore, $\text{PYRH}^+ \cdots \text{PYRH}^+$ dimers with pairs of H bonds between the N3 nitrogen and the 2-amino group are present. $\text{PYRH}^+\text{SAC}^-$ II (Figure S1) crystallizes in the triclinic space group P-1 in contrast to $\text{PYRH}^+\text{SAC}^-$ I which crystallizes in $P2_1/c$, but otherwise the two polymorphs of the anhydrous salt have very similar crystal structures. As in form I, two $\text{PYRH}^+ \cdots \text{SAC}^-$ heterodimers assemble through a pair of $\text{C2-NH}_2 \cdots \text{N3}$ H bonds and the resulting quartets are stacked along b . The quartet structures of forms I and II are further stabilized by $\text{C4-NH}_2 \cdots \text{O}=\text{S}$ H bonds. In both polymorphs, the second proton of the amino group at C4 does not form any H bond so that the H bonding interactions do not extend beyond the dimer of heterodimers motif. The two polymorphs of anhydrous $\text{PYRH}^+\text{SAC}^-$ differ in the dihedral angle between the phenyl and pyrimidine rings of PYRH^+ (87.65° in $\text{PYRH}^+\text{SAC}^-$ I vs. -70.65° in $\text{PYRH}^+\text{SAC}^-$ II).

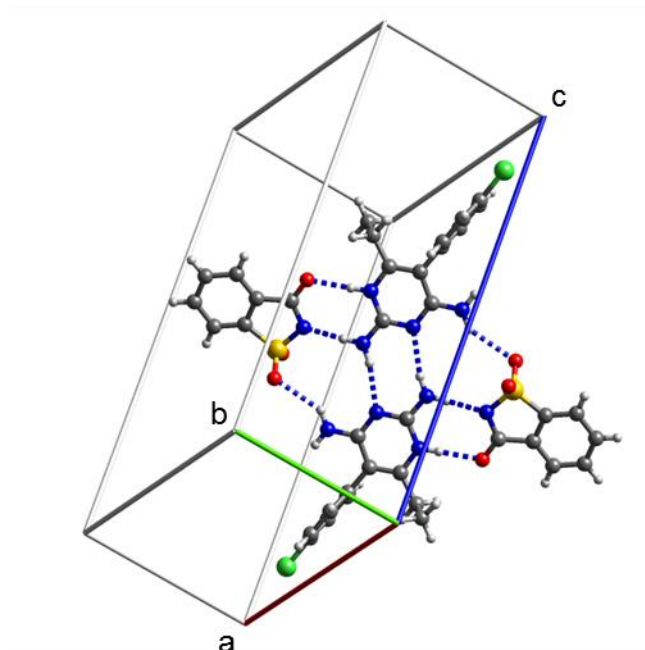


Figure 4. Hydrogen bonding motifs in the salt $\text{PYRH}^+\text{SAC}^-$ I obtained by sublimation.

X-ray Structure of $(\text{PYRH}^+\text{SAC}^-)_2\cdot\text{GLU}$. The structure of the ternary ionic cocrystal is shown in Figure 5. The asymmetric unit contains two PYRH^+ cations (PYRH^+ A and PYRH^+ B), two SAC^- anions (SAC^- A and SAC^- B) and one GLU molecule. The amide proton of SAC is transferred to the N1 nitrogen of PYR. The two crystallographically independent PYRH^+ cations adopt slightly different conformations with the dihedral angle between the pyrimidine and phenyl rings being 79.9 and 66.0 °, respectively. GLU forms three H bonds at the DAD site of PYRH^+ A. PYRH^+ B and SAC^- B interact *via* a pair of H bonds ($\text{N1H}^+\cdots\text{O}=\text{C}$, $\text{C2-NH}_2\cdots\text{N}^-$; $R_2^2(8)$ ring motif) as in the case of the binary $\text{PYRH}^+\text{SAC}^-$ salt. SAC^- A and PYRH^+ A also form two H bonds through the 2-aminopyrimidine site of PYRH^+ , however, H bonding is between N1H^+ and N^- and between $\text{C}=\text{O}$ and C2-NH_2 . A H bond between one of the sulfonyl oxygens and the second C2-NH_2 amino proton connects SAC^- A and PYRH^+ B. The PYRH^+ B cations are centrosymmetrically paired through two $\text{C4-NH}_2\cdots\text{N3}$ H bonds ($R_2^2(8)$ motif). The second amino proton of the amino group at C4 of both PYRH^+ does not participate in H bonding.

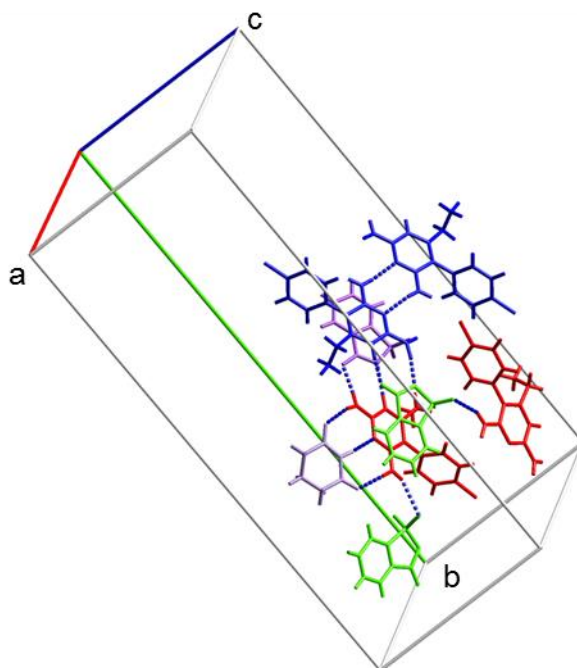


Figure 5. Hydrogen bonding motifs in the ternary ionic cocrystal $(\text{PYRH}^+\text{SAC}^-)_2\cdot\text{GLU}$. Red – PYR A, blue – PYR B, magenta – SAC A, green – SAC B, light magenta – GLU.

It is noteworthy that in all gas phase crystallizations except for $\text{PYR}\cdot\text{GLU}$ proton transfer takes place between the cofomer and PYR. As ions cannot form in the gas phase, the proton transfer must occur after the incorporation of the neutral species into the lattice. We have recently described the crystallization of zwitterionic *m*-aminobenzoic acid polymorphs from the gas phase and proposed that the formation of the zwitterions via proton transfer takes place during crystal growth.⁵⁵

Cocrystallization from Solution. Details of the solution crystallization experiments are summarized in Table S3. Two other ternary ionic cocrystals could be structurally characterized following crystallization from methanol; $(\text{PYRH}^+\text{BEN}^-)\cdot\text{PYR}\cdot\text{SUC}$ and $(\text{PYRH}^+\text{SAC}^-)_2\cdot\text{SOR}$. During attempts to obtain three-component crystals containing PYR, GLU and one of the carboxylic acids NIC, MAN or SOR the binary carboxylate salts $\text{PYRH}^+\text{NIC}^- \cdot 1.5\text{H}_2\text{O}$, $\text{PYRH}^+\text{MAN}^-$ and $\text{PYRH}^+\text{BEN}^- \cdot \text{H}_2\text{O}$ crystallized. $\text{PYRH}^+\text{BEN}^- \cdot \text{H}_2\text{O}$ has been recently characterized by single crystal X-ray analysis.⁵⁶ $\text{PYRH}^+\text{NIC}^- \cdot 1.5\text{H}_2\text{O}$ is different from the

monohydrate already reported in the literature²⁸ and the structure is described in the Supporting Information along with the structure of the new salt $\text{PYRH}^+\text{MAN}^-$ (Figures S2 and S3).

X-ray Structure of $(\text{PYRH}^+\text{BEN}^-)\cdot\text{PYR}\cdot\text{SUC}$. There are one PYRH^+ cation, one neutral PYR molecule, one SUC molecule and one benzoate anion in the asymmetric unit of $(\text{PYRH}^+\text{BEN}^-)\cdot\text{PYR}\cdot\text{SUC}$. SUC forms three hydrogen bonds with the C2-NH₂/N3/C4-NH₂ site of the (neutral) PYR molecule, while BEN^- interacts with the PYRH^+ cation at the protonated C2-NH₂/N1H⁺ site (Figure 6). One carbonyl oxygen of SUC accepts an additional H bond from the amino group at C4 of the PYRH^+ cation and one of the oxygens of BEN^- accepts a H bond from the 4-amino group of the neutral PYR molecule. The PYRH^+ cation and neutral PYR molecule interact with each other through the binding sites not occupied by a coformer *via* a pair of C2-NH₂...N1 and C2-NH₂...N3 H bonds.

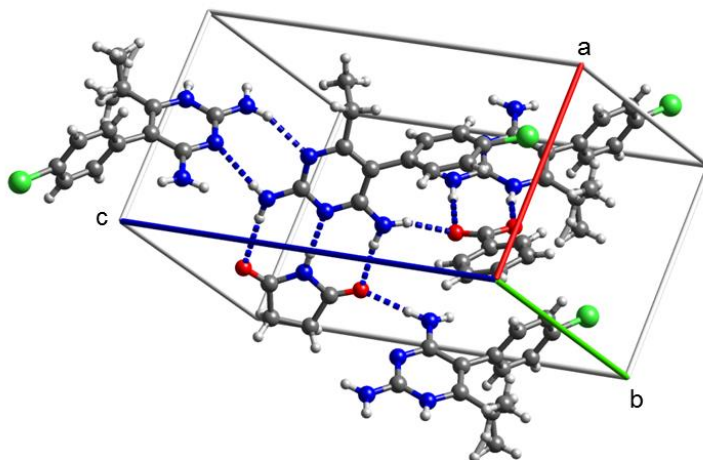


Figure 6. Hydrogen bonding motifs in the ternary ionic cocrystal $(\text{PYRH}^+\text{BEN}^-)\cdot\text{PYR}\cdot\text{SUC}$. For clarity, only one component of the disordered ethyl substituent on PYRH^+ is shown.

X-ray Structure of $(\text{PYRH}^+\text{SAC}^-)_2\cdot\text{SOR}$. The structure of the molecular ionic $(\text{PYRH}^+\text{SAC}^-)_2\cdot\text{SOR}$ cocrystal is shown in Figure 7. The asymmetric unit contains an N1-protonated PYRH^+ , a SAC^- anion and half a (neutral) SOR which is disordered about an inversion centre. The presence of deprotonated SAC and unde protonated SOR is consistent with

SAC being the stronger acid (pK_a of SAC and SOR = 1.6 and 4.8, respectively). The SAC^- anion forms two H bonds to the protonated 2-aminopyrimidine site with the deprotonated amide nitrogen of SAC^- interacting with $N1H^+$ and the amide oxygen interacting with the exocyclic amino group. The amide oxygen also accepts a H bond from the second 2-amino proton of a neighboring $PYRH^+$ which gives rise to $R_4^2(8)$ rings. Interactions between the amino protons at C4 of $PYRH^+$, both sulfonyl oxygens of SAC^- and the protonated carboxyl group of SOR generate $R_3^3(10)$ rings.

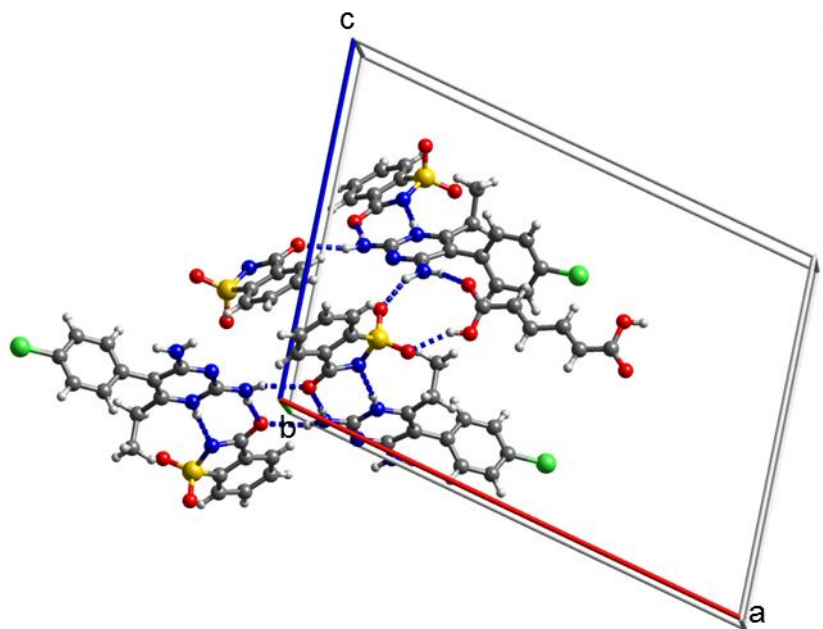


Figure 7. Hydrogen bonding motifs in the ternary ionic cocrystal $(PYRH^+SAC^-)_2 \cdot SOR$. For clarity only one component of the disordered SOR molecule is shown.

Investigation of Ternary Cocrystal Formation by Milling. As crystallization from the gas phase relies on the cosublimation of all three components and the outcome of solution crystallization experiments is determined by the relative solubilities of the ternary cocrystal, the single components and their solvates and the three possible two-component crystals, liquid-assisted milling was used as a wider screening method for ternary cocrystals of PYR.

Milling an equimolar mixture of PYR, SAC and GLU in the presence of traces of ethanol gave the ternary molecular ionic cocrystal as evidenced by comparison of the XRPD pattern with the theoretical pattern calculated from the single crystal data of $(\text{PYRH}^+\text{SAC}^-)_2\cdot\text{GLU}$ (Figure 8).

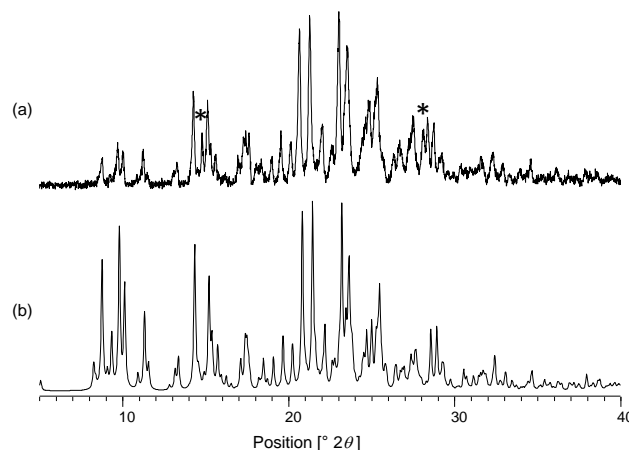


Figure 8. (a) XRPD patterns of a milled sample of PYR, GLU and SAC (1:1:1 molar ratio) and (b) the theoretical pattern of the ternary $(\text{PYRH}^+\text{SAC}^-)_2\cdot\text{GLU}$ cocrystal calculated from the single crystal data. * unreacted GLU.

The same experiment with mixtures of PYR, GLU and SOR and PYR, GLU and MAN (1:1:1 molar ratio) showed the respective PYR-carboxylate salts only (Figures S4 and S5). $\text{PYRH}^+\text{MAN}^-$ as the reaction product was confirmed by calculating the XRPD pattern from the single crystal structure obtained during the unsuccessful attempts to crystallize a ternary cocrystal from solution (see above). To identify the sorbate salt, single crystals were prepared by cocrystallizing PYR and SOR from solution (Figure S6). The XRPD pattern of a milled PYR/GLU/NIC sample showed the Bragg peaks of unreacted GLU, traces of $\text{PYR}\cdot\text{GLU}$ and a main product. The peaks of the main product did not match the simulated pattern of the anhydrous PYR-NIC salt obtained by sublimation or those of $\text{PYRH}^+\text{NIC}^-\cdot\text{H}_2\text{O}^{28}$ or $\text{PYRH}^+\text{NIC}^-\cdot 1.5\text{H}_2\text{O}$. However, the same peaks were observed, when a binary mixture of PYR and NIC was

milled (Figure S7) suggesting that the main product in the milled PYR/GLU/NIC sample is a different polymorph or pseudopolymorph of $\text{PYRH}^+\text{NIC}^-$.

In all cases the same results were obtained, when the mechanochemical reaction was carried out stepwise (Figures S4, S5 and S7). Milling PYR with the respective carboxylic acid first gave $\text{PYRH}^+\text{SOR}^-$, $\text{PYRH}^+\text{MAN}^-$ and the unknown PYR/NIC crystal and no reaction took place on milling the binary systems with GLU. Preparing the PYR·GLU cocrystal first and adding the carboxylic acid in the second step resulted in the release of GLU.

Milling PYR, BEN and GLU together gave a new XRPD pattern that was different from that of the binary cocrystals $\text{PYRH}^+\text{BEN}^- \cdot \text{H}_2\text{O}$ and PYR·GLU (Figure S8). This new pattern was also obtained, when the coformers were added stepwise (PYR/BEN + GLU and PYR/GLU + BEN). No Bragg peaks of PYR were observed and the new XRPD pattern may indicate the formation of a ternary cocrystal. However, a mixture cannot be excluded. Attempts to crystallize the PYR/BEN/GLU system from solution by dissolving the milled sample in the hope that seeds of the potential ternary cocrystal may influence the crystallization process led to crystals of the $\text{PYRH}^+\text{BEN}^-$ hydrate only.

Two-component cocrystals were formed on milling PYR/BAR/NIC, PYR/BAR/MAN and PYR/BAR/SOR (Figures S9 – S11). As found for the PYR/GLU/carboxylic acid systems the nature of the respective product was independent on the milling procedure (one-step, two-step, order of addition). In the PYR/BAR/NIC and PYR/BAR/SOR mixtures, the ADA coformer formed the cocrystal with PYR. The XRPD pattern of milled PYR/BAR/NIC is different from the simulated pattern of the ionic cocrystal $\text{PYRH}^+\text{BAR}^- \cdot \text{PYR}$ but matches the pattern obtained after milling a binary mixture of PYR and BAR. By contrast the PYR/BAR/MAN mixture converted to the $\text{PYRH}^+\text{MAN}^-$ salt. The XRPD patterns of the milling experiments with BEN are less conclusive (Figure S12) and may represent mixtures of different solid-state forms.

The XRPD pattern of an equimolar mixture of PYR and SUC after milling was that of a physical mixture and no further milling experiments were carried out with this coformer. The results of all milling experiments are summarized in Scheme 1.

milling product independent on milling procedure		
ADA coformer	AD coformer	milling product
GLU	SAC	ternary cocrystal
	SOR	binary cocrystal with the AD coformer
	MAN	binary cocrystal with the AD coformer
	NIC	binary cocrystal with the AD coformer
	BEN	unknown, possibly ternary cocrystal
BAR	NIC	binary cocrystal with the ADA coformer
	SOR	binary cocrystal with the ADA coformer
	MAN	binary cocrystal with the AD coformer
	BEN	unknown, possibly mixture
competition experiments with SAC		
	BEN MAN	PYRH ⁺ SAC ⁻ II PYRH ⁺ MAN ⁻
milling product dependent on milling procedure		
competition experiments with SAC		
	SOR NIC	<pre> graph LR A[SAC/SOR SAC/NIC] -- one-pot --> B[PYRH+SAC- II] A -- stepwise --> C[1. SAC] C --> B B -- 2. SOR/NIC --> D[unknown product] A -- stepwise --> E[1. SOR/NIC] E --> F[PYRH+SOR- PYR/NIC] F -- 2. SAC --> G[unknown product] </pre>

Scheme 1. Results of the milling experiments with pyrimethamine and different ADA and AD coformers.

Competition of SAC and Carboxylic Acids for the 2-Aminopyrimidine Site of PYR. As both, SAC and carboxylic acids, interact with the 2-aminopyrimidine site of PYR, PYR was milled with SAC and one mole equivalent of SOR, BEN, MAN or NIC. In each case the two coformers were mixed and milled with PYR as a one-pot reaction, in two steps with SAC being added first and in two steps with the carboxylic acid being added first. In addition, solution crystallization experiments were carried out.

The XRPD patterns of the milled ternary mixtures PYR/SAC/NIC and PYR/SAC/BEN showed PYRH⁺SAC⁻ II as the only product of the one-pot reaction (Figures S13 and S14), while the mixture of PYR, SAC and MAN converted to the binary PYRH⁺MAN⁻ salt (Figure S15, Scheme

1). In the case of the PYR/SAC/BEN and PYR/SAC/MAN systems, the SAC and MAN cocrystals also formed when the coformers were added stepwise, independent on the order of addition (Figure S13 and S15). By contrast, for the mechanochemical reaction between PYR, SAC and NIC and between PYR, SAC and SOR, the order in which the coformers were added was important in the stepwise milling experiment. When PYR was milled first with SAC, $\text{PYRH}^+\text{SAC}^-$ II was formed and no further transformation was observed in the second milling step with the carboxylic acid. However, addition of SAC to PYR/NIC or PYR/SOR in the second milling step gave yet unknown products (Figures S14 and S16). In the case of PYR/SOR/SAC, the XRPD pattern did not match the simulated pattern calculated from the single crystal data of the ternary cocrystal. However, a different polymorph or stoichiometry cannot be excluded.

Crystallization from solution yielded four new solid-state structures of $\text{PYRH}^+\text{SAC}^-$: Cocrystallization of PYR and SAC from methanol gave a new polymorph of the methanol solvate reported in the literature.³⁸ Using acetonitrile as the solvent yielded the solvate $\text{PYRH}^+\text{SAC}^- \cdot \text{CH}_3\text{CN}$. The hydrates $\text{PYRH}^+\text{SAC}^- \cdot \text{H}_2\text{O}$ and $\text{PYRH}^+\text{SAC}^- \cdot 2.2\text{H}_2\text{O}$ were obtained by slow evaporation of a methanol solution containing equimolar amounts of PYR, SAC and NIC and PYR, SAC and MAN, respectively. Anhydrous $\text{PYRH}^+\text{SAC}^-$ II crystallized from solutions of the milled PYR/SAC/SOR mixture. However, it has to be noted that XRPD analysis indicated that the crystal structures of the methanol solvate polymorph and of the hydrates were not representative of the bulk samples.

X-ray Structures of $\text{PYRH}^+\text{SAC}^- \cdot \text{CH}_3\text{OH}$ II, $\text{PYRH}^+\text{SAC}^- \cdot \text{CH}_3\text{CN}$, $\text{PYRH}^+\text{SAC}^- \cdot \text{H}_2\text{O}$, and $\text{PYRH}^+\text{SAC}^- \cdot 2.2\text{H}_2\text{O}$. The X-ray structures of $\text{PYRH}^+\text{SAC}^- \cdot \text{CH}_3\text{OH}$ II, $\text{PYRH}^+\text{SAC}^- \cdot \text{CH}_3\text{CN}$, $\text{PYRH}^+\text{SAC}^- \cdot \text{H}_2\text{O}$, and $\text{PYRH}^+\text{SAC}^- \cdot 2.2\text{H}_2\text{O}$ are shown in Figures S17 – S20. The previously described solvated salt $\text{PYRH}^+\text{SAC}^- \cdot \text{CH}_3\text{OH}$ features an $R_4^2(8)$ motif created by two $\text{PYRH}^+\text{SAC}^-$ heterodimers.³⁸ This motif is absent in $\text{PYRH}^+\text{SAC}^- \cdot \text{CH}_3\text{OH}$ II. Instead, two heterodimers are linked through pairwise C4-NH₂...N3 H bonding ($R_2^2(8)$). In the polymorph reported previously, two adjacent dimers of heterodimers are linked through methanol of crystallization that interacts with a sulfonyl oxygen of SAC^- and the 4-amino group of PYRH^+ , while in $\text{PYRH}^+\text{SAC}^- \cdot \text{CH}_3\text{OH}$ II the methanol stabilizes the PYRH^+ - PYRH^+ homosynthon by interacting with the amino groups at the C2 and C4 sites and donates a H bond to the sulfonyl

group of an adjacent SAC^- . The acetonitrile solvate and the monohydrate of $\text{PYRH}^+\text{SAC}^-$ have the same quartet motif as $\text{PYRH}^+\text{SAC}^- \cdot \text{CH}_3\text{OH}$ I. The $\text{S}=\text{O} \cdots \text{HO}(\text{CH}_3) \cdots \text{H}_2\text{N}-\text{C}_4$ H bonding motif is replaced by a direct $\text{S}=\text{O} \cdots \text{H}_2\text{N}-\text{C}_4$ interaction in $\text{PYRH}^+\text{SAC}^- \cdot \text{CH}_3\text{CN}$. The acetonitrile nitrogen accepts a H bond from the 4-amino group of PYRH^+ . In the crystal structure of the monohydrate two water molecules of crystallization and two SAC^- anions assemble into a 12-membered ring with the water molecules donating H bonds to sulfonyl oxygen ($R_4^4(12)$ motif). The water molecule also accepts a H bond from the amino group at C4 of an adjacent PYRH^+ . In $\text{PYRH}^+\text{SAC}^- \cdot 2.2\text{H}_2\text{O}$ 1.2 water molecules of crystallization are disordered over three positions with site occupancies of 0.6, 0.4 and 0.2. The H bonding between SAC^- and PYRH^+ is between the protonated N1 of PYRH^+ and the deprotonated nitrogen in SAC^- and between the 2-amino group and the amide oxygen in $\text{PYRH}^+\text{SAC}^- \cdot \text{CH}_3\text{OH}$ II, $\text{PYRH}^+\text{SAC}^- \cdot \text{CH}_3\text{CN}$, and $\text{PYRH}^+\text{SAC}^- \cdot \text{H}_2\text{O}$, while in $\text{PYRH}^+\text{SAC}^- \cdot 2.2\text{H}_2\text{O}$ it is the same as in the anhydrous $\text{PYRH}^+\text{SAC}^-$ polymorphs (i.e. between the protonated N1 in PYRH^+ and the amide oxygen of SAC^- and between the 2-amino group and N^- of SAC^-).

Thermal Analysis and PIXEL Calculations. In order to investigate the stabilities of the PYR-ADA coformer and PYR-AD coformer interactions and to rationalize the outcomes of the milling experiments DSC measurements (Figures S21 – S25) and PIXEL calculations⁵⁷ were carried out, with bonds to hydrogen set at neutron diffraction values, and the contributions of the different interactions toward the stability of the binary cocrystals $\text{PYRH}^+\text{MAN}^-$, $\text{PYR} \cdot \text{GLU}$, $\text{PYRH}^+\text{SOR}^-$, and $\text{PYRH}^+\text{SAC}^-$ I and II were analyzed (Supporting Information). The ternary cocrystals have $Z' > 2$ which is beyond the computational limitations of the PIXEL programme.

The only thermal event in the thermogram of $\text{PYRH}^+\text{MAN}^-$ is the melting of the salt at 215.9 °C. The DSC plot of $\text{PYR} \cdot \text{GLU}$ shows a melting endotherm at 185.7 °C followed by melting of PYR at 240.7 °C. A higher melting point is usually associated with a higher lattice energy. PIXEL calculations gave lattice energies of -171.3 and -124.8 kJ mol^{-1} for $\text{PYRH}^+\text{MAN}^-$ and $\text{PYR} \cdot \text{GLU}$, respectively. The strongest interaction in the solid-state structure of $\text{PYR} \cdot \text{GLU}$ is the interaction of the coformer at the C2-NH₂/N3/C4-NH₂ site with an interaction energy of -65.4 kJ mol^{-1} . This compares to -98.7 kJ mol^{-1} for the interaction between PYRH^+ and MAN^- involving charge assisted H bonding at the C-NH₂/N1 site. The second strongest interaction in the $\text{PYR} \cdot \text{GLU}$

cocrystal is the C2-NH₂...N1 homosynthon (interaction energy -56.2 kJ mol⁻¹). The PYR...PYR homosynthon is absent in PYRH⁺MAN⁻. There are two strong interactions of -51.5 and -47.6 kJ mol⁻¹ that are dominated by a bifurcated NH...O/OOC H bond and an OH...O H bond between two MAN⁻ anions, respectively. Hence, the PIXEL calculations confirm that milling a mixture of PYR, GLU and MAN gives the binary cocrystal with the more negative lattice energy. The same is true for the PYR/GLU/SOR system. The lattice energy of PYRH⁺SOR⁻ was calculated as -162.7 kJ mol⁻¹. Again, the dominant contribution is the charge-assisted H bond between the carboxylate group of SOR and the pyrimidine site of PYR (interaction energy -80.7 kJ mol⁻¹). The DSC/TGA plot of PYRH⁺SOR⁻ shows an endotherm at 170.9 °C accompanied by a weight loss which is assigned to the decomposition of sorbic acid.⁵⁸

MAN is the only acid that competes with BAR for forming a binary cocrystal with PYR. It is noteworthy that MAN has the lowest pK_a value of all the carboxylic acids used in the study. In contrast to GLU, BAR interacts in its anionic form with the C2-NH₂/N3/C4-NH₂ site of PYR. Unfortunately, PIXEL calculations are not possible for the PYR-BAR system as the structure of the milling product is not known and the structure of PYRH⁺BAR⁻·PYR obtained by sublimation has Z' > 2.

As discussed above, the two polymorphs of anhydrous PYRH⁺SAC⁻ have the same H bonding motif. In the DSC plot of PYRH⁺SAC⁻ I, a small endotherm at 212.6 °C is observed followed by melting at 223.1 °C. The endotherm at 212.6 °C is assigned to the transformation to form II. Given the similarity of the structures of PYRH⁺SAC⁻ I and II, the transition enthalpy should be small. The strongest interactions in the solid-state structures of forms I and II are the PYRH⁺...SAC⁻ R₂²(8) heterosynthon and the PYR...PYR R₂²(8) homosynthon with interaction energies of 60 – 65 kJ mol⁻¹, dominated by H bonding. The main difference between the polymorphs is the contribution of a strong van der Waals interaction of -46.8 kJ mol⁻¹ between PYRH⁺ and SAC⁻ of two adjacent (PYRH⁺...SAC⁻)...(PYRH⁺...SAC⁻) quartets in form II.

CONCLUSIONS

Our study further confirms that two-zone cosublimation is a viable alternative to solution crystallization for the preparation of high-quality single cocrystals. Cosublimation and solution cocrystallization of PYR with NIC give different polymorphs/pseudopolymorphs of the salt cocrystal. In the case of PYR/BAR a molecular ionic cocrystal can be obtained by sublimation that is not accessible from solution due to the poor solubility of the coformer. Careful experimental design even allows the crystallization of a three-component crystal from the gas phase. The three preparation methods of cocrystals used in this work, sublimation, solution crystallization and liquid-assisted milling are compared in Table 2.

Out of the three ternary cocrystals that could be structurally characterized only $(\text{PYRH}^+\text{SAC}^-)_2\cdot\text{GLU}$ shows the anticipated interaction of both coformers with the same PYR molecule. By contrast, in $(\text{PYRH}^+\text{BEN}^-)\cdot\text{PYR}\cdot\text{SUC}$, the ADA and AD coformer bind to their respective binding site in two different PYR molecules/ions. Binding of SAC and carboxylic acid at the 2-aminopyrimidine site is accompanied by proton transfer resulting in the formation of a strong charge-assisted H bond. H bonding between the ADA coformer and the C2-NH₂/N3/C4-NH₂ site will affect the basicity of the N1 nitrogen. SAC ($\text{pK}_a = 1.6$) is a stronger acid than BEN ($\text{pK}_a = 4.2$) which may explain the $(\text{PYRH}^+\text{SAC}^-)_2\cdot\text{GLU}$ and $(\text{PYRH}^+\text{BEN}^-)\cdot\text{PYR}\cdot\text{SUC}$ compositions of the two ternary systems.

$(\text{PYRH}^+\text{SAC}^-)_2\cdot\text{GLU}$ is the only ternary molecular ionic cocrystal that could be prepared by milling. The ternary mixtures containing a carboxylic acid as the AD coformer all transform to a binary cocrystal/salt. PIXEL calculations confirm that of the two coformers (ADA or DA coformer) the one that gives the cocrystal with the higher lattice energy reacts with PYR in the mechanochemical reaction. Competition experiments with SAC and carboxylic acid coformers show a preference of the 2-aminopyrimidine site of PYR to interact with the anion of the more acidic SAC, the only exception being the preferred formation of the $\text{PYRH}^+\text{MAN}^-$ salt which has the lowest pK_a value of all the carboxylic acids used in the study. Various new solid-state forms of $\text{PYRH}^+\text{SAC}^-$ could be obtained and there is no obvious preference for the orientation of SAC^- in the $R_2^2(8)$ motif, i.e. $\text{N1H}^+\cdots\text{O}=\text{C}/\text{C2-NH}_2\cdots\text{N}^-$ vs. $\text{N1H}^+\cdots\text{N}^-/\text{C2-NH}_2\cdots\text{O}=\text{C}$ H bonding.

SUPPORTING INFORMATION

Experimental details of the ball milling and solution crystallization experiments; crystal data of $\text{PYRH}^+\text{NIC}^- \cdot 1.5\text{H}_2\text{O}$, $\text{PYRH}^+\text{MAN}^-$, $\text{PYRH}^+\text{SOR}^-$, $\text{PYRH}^+\text{SAC}^- \cdot \text{H}_2\text{O}$, $\text{PYRH}^+\text{SAC}^- \cdot 2.2\text{H}_2\text{O}$, $\text{PYRH}^+\text{SAC}^- \cdot \text{CH}_3\text{OH}$ and $\text{PYRH}^+\text{SAC}^- \cdot \text{CH}_3\text{CN}$; H bonding interactions; description of the X-ray structures of $\text{PYRH}^+\text{NIC}^- \cdot 1.5\text{H}_2\text{O}$, $\text{PYRH}^+\text{MAN}^-$, and $\text{PYRH}^+\text{SOR}^-$; measured and calculated XRPD patterns; DSC plots and details of the PIXEL calculations.

ACKNOWLEDGEMENTS

This publication has emanated from research supported in part by a research grant from Science Foundation Ireland (SFI) and is co-funded under the European Regional Development Fund under Grant Number 12/RC/2275.

REFERENCES

- (1) Shan, N.; Zaworotko, M. J. The role of cocrystals in pharmaceutical science. *Drug Discov. Today* **2008**, *13*, 440–446.
- (2) Shunnar, A. F.; Dhokale, B.; Karothu, D. P.; Bowskill, D. H.; Sugden, I. J.; Hernandez, H. H.; Naumov, P.; Mohamed, S. Efficient screening for ternary molecular ionic cocrystals using a complementary mechanosynthesis and computational structure prediction approach. *Chem. Eur. J.* **2020**, *26*, 4752–4765.
- (3) Aakeröy, C. B.; Desper, J.; Fasulo, M.; Hussain, I.; Levin, B.; Schultheiss, N. Ten years of co-crystal synthesis; the good, the bad, and the ugly. *CrystEngComm* **2008**, *10*, 1816–1821.
- (4) Aakeröy, C. B.; Beatty, A. M.; Helfrich, B. A. “Total Synthesis” supramolecular style: Design and hydrogen-bond-directed assembly of ternary supermolecules. *Angew. Chem. Int. Ed.* **2001**, *40*, 3240–3242.

- (5) Aakeröy, C. B.; Desper, J.; Urbina, J. F. Supramolecular reagents: versatile tools for non-covalent synthesis. *Chem. Commun.* **2005**, 2820–2822.
- (6) Tothadi, S.; Desiraju, G. R. Designing ternary cocrystals with hydrogen bonds and halogen bonds. *Chem. Commun.* **2013**, 49, 7791–7793.
- (7) Topic, F.; Rissanen, K. Systematic construction of ternary cocrystals by orthogonal and robust hydrogen and halogen bonds. *J. Am. Chem. Soc.* **2016**, 138, 6610–6616.
- (8) Gunawardana, C. A.; Aakeröy, C. B. Co-crystal synthesis: fact, fancy, and great expectations. *Chem. Commun.* **2018**, 54, 14047–14060.
- (9) Aakeröy, C. B.; Desper, J.; Smith, M. M. Constructing, deconstructing, and reconstructing ternary supermolecules. *Chem. Commun.* **2007**, 3936–3938.
- (10) Adsmund, D. A.; Sinha, A. S.; Khandavilli, U. B. R.; Maguire, A. R.; Lawrence, S. E. Design and synthesis of ternary cocrystals using carboxyphenols and two complementary acceptor compounds. *Cryst. Growth Des.* **2016**, 16, 59–69.
- (11) Tothadi, S.; Mukherjee, A.; Desiraju, G. R. Shape and size mimicry in the design of ternary molecular solids: towards a robust strategy for crystal engineering. *Chem. Commun.* **2011**, 47, 12080–12082.
- (12) Dubey, R.; Desiraju, G. R. Combinatorial crystal synthesis: Structural landscape of phloroglucinol:1,2-bis(4-pyridyl)ethylene and phloroglucinol:phenazine. *Angew. Chem. Int. Ed.* **2014**, 53, 13178–13182.
- (13) Mir, N. A.; Dubey, R.; Tothadi, S.; Desiraju, G. R. Combinatorial crystal synthesis of ternary solids based on 2-methylresorcinol. *CrystEngComm* **2015**, 17, 7866–7869.
- (14) Tothadi, S.; Sanphui, P.; Desiraju, G. R. Obtaining synthon modularity in ternary cocrystals with hydrogen bonds and halogen bonds. *Cryst. Growth Des.* **2014**, 14, 5293–5302.
- (15) Aitipamula, S.; Wong, A. B. H.; Choi, P. S.; Tan, R. B. H. Novel solid forms of the anti-tuberculosis drug, isoniazid: ternary and polymorphic cocrystals. *CrystEngComm* **2013**, 15, 5877–5887.

- (16) Portalone, G.; Rissanen, K. Multifacial recognition in binary and ternary cocrystals from 5-halouracil and aminoazine derivatives. *Cryst. Growth Des.* **2018**, *18*, 5904–5918.
- (17) Liu, F.; Song, Y.; Liu, Y.-N.; Li, Y.-T.; Wu, Z.-Y.; Yan, C.-W. Drug-Bridge-Drug ternary cocrystallization strategy for antituberculosis drugs combination. *Cryst. Growth Des.* **2018**, *18*, 1283–1286.
- (18) Dubey, R.; Desiraju, G. R. Combinatorial selection of molecular conformations and supramolecular synthons in quercetin cocrystal landscapes: a route to ternary solids. *IUCrJ* **2015**, *2*, 402–408.
- (19) Seaton, C. C.; Blagden, N.; Munshi, T.; Scowen, I. J. Creation of ternary multicomponent crystals by exploitation of charge-transfer interactions. *Chem. Eur. J.* **2013**, *19*, 10663–10671.
- (20) Frisic, T.; Trask, A. V.; Jones, W.; Motherwell, W. D. S. Screening for inclusion compounds and systematic construction of three-component solids by liquid-assisted grinding. *Angew. Chem. Int. Ed.* **2006**, *45*, 7546–7550.
- (21) Bhogola, B. R.; Basavoju, S.; Nangia, A. Three-component carboxylic acid–bipyridine lattice inclusion host. Supramolecular synthesis of ternary cocrystals. *Cryst. Growth Des.* **2005**, *5*, 1683–1686.
- (22) Etter, M. C. Encoding and decoding hydrogen-bond patterns of organic compounds. *Acc. Chem. Res.* **1990**, *23*, 120–126.
- (23) Mir, N. A.; Dubey, R.; Desiraju, G. R. Four- and five-component molecular solids: crystal engineering strategies based on structural inequivalence. *IUCrJ* **2016**, *3*, 96–101.
- (24) Dubey, R.; Mir, N. A.; Desiraju, G. R. Quaternary cocrystals: combinatorial synthetic strategies based on long-range synthon Aufbau modules (LSAM). *IUCrJ* **2016**, *3*, 102–107.
- (25) Paul, M.; Chakraborty, S.; Desiraju, G. R. Six-component molecular solids: ABC[D₁–_(x+y)E_xF_y]₂. *J. Am. Chem. Soc.* **2018**, *140*, 2309–2315.

- (26) Stanley, N.; Sethuraman, V.; Muthiah, P. T.; Luger, P.; Weber, M. Crystal engineering of organic salts: hydrogen-bonded supramolecular motifs in pyrimethamine hydrogen glutarate and pyrimethamine formate. *Cryst. Growth Des.* **2002**, *2*, 631–635.
- (27) Sethuraman, V.; Stanley, N.; Muthiah, P. T.; Sheldrick, W. S.; Winter, M.; Luger, P.; Weber, M. Isomorphism and crystal engineering: organic ionic ladders formed by supramolecular motifs in pyrimethamine salts. *Cryst. Growth Des.* **2003**, *3*, 823–828.
- (28) Balasubramani, K.; Muthiah, P. T.; Bocelli, G.; Cantoni, A. Pyrimethaminium nicotinate monohydrate. *Acta Cryst.* **2007**, *E63*, o4452.
- (29) Balasubramani, K.; Muthiah, P. T. Hydrogen-bonding patterns in pyrimethaminium picolinate. *Anal. Sc.* **2008**, *24*, 251–252.
- (30) Devi, P.; Muthiah, P. T.; Guru Row, T. N.; Thiruvengatam, V. Hydrogen bonding in pyrimethamine hydrogen adipate. *Acta Cryst.* **2007**, *E63*, o4065–o4066.
- (31) Stanley, N.; Muthiah, P. T.; Geib, S. J.; Luger, P.; Weber, M.; Messerschmidt, M. The novel hydrogen bonding motifs and supramolecular patterns in 2,4-diaminopyrimidine-nitrobenzoate complexes. *Tetrahedron*, **2005**, *61*, 7201–7210.
- (32) Natarajan, S.; Mathews, R. 2,4-diamino-5-(4-chlorophenyl)-6-ethyl-pyrimidin-1-ium 2 acetamidebenzoate. *Acta Cryst.* **2011**, *E67*, o2357–o2358.
- (33) Faroque, M. U.; Noureen, S.; Mirza, S. H.; Tahir, M. N.; Ahmed, M. Structure and electrostatic properties of the pyrimethamine-3,5-dihydroxybenzoic acid cocrystal in water solvent studied using transferred electron-density parameters. *Acta Cryst.* **2019**, *C75*, 46–53.
- (34) Tahir, M. N.; Mirza, S. H.; Khalid, M.; Ali, A.; Khan, M. U.; Braga, A. A. C., Synthesis, single crystal analysis and DFT based computational studies of 2,4-diamino-5-(4-chlorophenyl)-6-ethylpyrimidin-1-ium 3,4,5-trihydroxybenzoate-methanol (DETM). *J. Mol. Struct.* **2019**, *1180*, 119–126.
- (35) Yamuna, T. S.; Kaur, M.; Jasinski, J. P.; Yathirajan, H. S. Pryrimethaminium 2-[[4-(trifluoromethyl)phenyl]sulfanyl]benzoate dimethyl sulfoxide monosolvate. *Acta Cryst.* **2014**, *E70*, o683–o684.

- (36) Delori, A.; Galek, P. T. A.; Pidcock, E.; Jones, W. Quantifying homo- and heteromolecular hydrogen bonds as a guide for adduct formation. *Chem. Eur. J.* **2012**, *18*, 6835–6846.
- (37) Faroque, M. U.; Noureen, S.; Ahmed, M.; Tahir, M. N. Electrostatic properties of the pyrimethamine-2,4-dihydroxybenzoic acid cocrystal in methanol studied using transferred electron-density parameters. *Acta Cryst.* **2018**, *C74*, 100–107.
- (38) Delori, A.; Galek, P. T. A.; Pidcock, E.; Patni, M.; Jones, W. Knowledge-based hydrogen bond prediction and the synthesis of salts and cocrystals of the anti-malarial drug pyrimethamine with various drug and GRAS molecules. *CrystEngComm* **2013**, *15*, 2916–2928.
- (39) Nirmalram, J. S.; Muthiah, P. T. Hydrogen-bonding patterns in pyrimethaminium pyridine-3-sulfonate. *Acta Cryst.* **2010**, *E66*, o2121–o2122.
- (40) Hemamalini, M.; Muthiah, P. T.; Sridhar, B.; Rajaram, R. K. Pyrimethaminium sulfosalicylate monohydrate. *Acta Cryst.* **2005**, *E61*, o1480–o1482.
- (41) Nakai, H.; Takasuka, M.; Shiro, M. X-ray and infrared spectral studies of the ionic structure of trimethoprim-sulfamethoxazole 1:1 molecular complex. *J. Chem. Soc. Perkin Trans. II* **1984**, 1459–1464.
- (42) Giuseppetti, G.; Tadini, C. 1:1 Molecular complex of trimethoprim and sulfametrole. *Acta Cryst.* **1994**, *C50*, 1289–1291.
- (43) Bettinetti, G.; Caira, M. R.; Callegari, A.; Merli, M.; Sorrenti, M.; Tadini, C. Structure and solid-state chemistry of anhydrous and hydrated crystal forms of the trimethoprim-sulfamethoxypyridazine 1:1 molecular complex. *J. Pharm. Sci.* **2000**, *89*, 478–489.
- (44) Bettinetti, G.; Sardone, N. Methanol solvate of the 1:1 molecular complex of trimethoprim and sulfadimidine. *Acta Cryst.* **1997**, *C53*, 594–597.
- (45) Sardone, N.; Bettinetti, G.; Sorrenti, M. Trimethoprim-sulfadimidine 1:2 molecular complex monohydrate. *Acta Cryst.* **1997**, *C53*, 1295–1299.
- (46) Brittain, H.G. Polymorphism in pharmaceutical solids. In Swarbrick, J. Ed. *Drugs and the Pharmaceutical Sciences*. New York: Informa Healthcare **2009**, pp186–188.

- (47) Karpinska, J.; Erxleben, A.; McArdle, P. 17β -hydroxy- 17α -methylandro-stano[3,2-c]-pyrazole, Stanazolol: The crystal structures of polymorphs 1 and 2 and ten solvates. *Cryst. Growth Des.* **2011**, *11*, 2829–2838.
- (48) Karpinska, J.; Erxleben, A.; McArdle, P. Applications of low temperature gradient sublimation in vacuo: Rapid production of high quality crystals; the first solvent-free crystals of ethinyl estradiol. *Cryst. Growth Des.* **2013**, *13*, 1122–1130.
- (49) Szell, P. M. J.; Gabriel, S. A.; Caron-Poulin, E.; Jeannin, O.; Fourmigue, M.; Bryce, D. L. Cosublimation: A rapid route towards otherwise inaccessible halogen-bonded architectures. *Cryst. Growth Des.* **2018**, *18*, 6227–6238.
- (50) Carstens, T.; Haynes, D. A.; Smith, V. J. Cocrystals: Solution, mechanochemistry, and sublimation. *Cryst. Growth Des.* **2020**, *20*, 1139–61149.
- (51) O'Malley, C.; Erxleben, A.; Kellehan, S.; McArdle, P. Unprecedented morphology control of gas phase cocrystal growth using multi zone heating and tailor made additives. *ChemComm.* **2020**, *56*, 5657–5660.
- (52) McArdle, P. Oscail, a Program Package for Small-Molecule Single-Crystal Crystallography with Crystal Morphology Prediction and Molecular Modelling. *J. Appl. Cryst.* **2017**, *50*, 320–326.
- (53) Sheldrick, G. M. SHELXT - Integrated space-group and crystal-structure determination. *Acta Cryst.* **2015**, *A71*, 3–8.
- (54) Sheldrick, G. M. Crystal structure refinement with SHELXL. *Acta Cryst.* **2015**, *A71*, 3–8.
- (55) Kamali, N.; O'Malley, C.; Mahon, M. F.; Erxleben, A.; McArdle, P. Use of sublimation catalysis and polycrystalline powder templates for polymorph control of gas phase crystallization. *Cryst. Growth Des.* **2018**, *18*, 3510–3516.
- (56) Faroque, M. U.; Mehmood, A.; Noureen, S.; Ahmed, M. Crystal engineering and electrostatic properties of co-crystals of pyrimethamine with benzoic acid and gallic acid. *J. Mol. Struct.* **2020**, *1214*, 128183.

(57) Gavezzotti, A. Calculation of lattice energies of organic crystals:the PIXEL integration method in comparison with more traditionalmethods. *Z. Kristallogr. - Cryst. Mater.* **2005**, *220*, 499–510.

(58) Reda, S. Y. Evaluation of antioxidants stability by thermal analysis and its protective effect in heated edible vegetable oil. *Ciênc. Tecnol. Aliment.* **2011**, *31*, 475–480.

Table 1. Crystal data of the binary and ternary salts and cocrystals PYR·GLU, PYRH⁺BAR⁻·PYR, PYRH⁺NIC⁻, PYRH⁺SAC⁻ I, PYRH⁺SAC⁻ II, (PYRH⁺SAC⁻)₂·GLU, (PYRH⁺BEN⁻)·PYR·SUC and (PYRH⁺SAC⁻)₂·SOR.

	PYR·GLU	PYRH ⁺ BAR ⁻ ·PYR	PYRH ⁺ NIC ⁻	PYRH ⁺ SAC ⁻ I	PYRH ⁺ SAC ⁻ II	(PYRH ⁺ SAC ⁻) ₂ ·GLU	(PYRH ⁺ BEN ⁻)·PYR·SUC	(PYRH ⁺ SAC ⁻) ₂ ·SOR
Formula	C ₁₇ H ₂₀ ClN ₅ O ₂	C ₂₈ H ₃₀ Cl ₂ N ₁₀ O ₃	C ₁₈ H ₁₈ ClN ₅ O ₂	C ₁₉ H ₁₈ ClN ₅ O ₃ S	C ₁₉ H ₁₈ ClN ₅ O ₃ S	C ₄₃ H ₄₃ Cl ₂ N ₁₁ O ₈ S ₂	C ₃₅ H ₃₇ Cl ₂ N ₉ O ₄	C ₂₂ H ₂₂ ClN ₅ O ₄ S
<i>M</i> _r	361.83	625.52	371.82	431.89	431.89	976.90	718.63	487.95
Crystal colour and habit	Colourless Plate	Colourless Plate	Colourless Plate	Colourless Needle	Colourless Plate	Colourless Plate	Colourless Plate	Colourless Needle
Crystal size (mm)	0.3 x 0.3 x 0.15	0.4 x 0.4 x 0.05	0.9 x 0.8 x 0.3	0.9 x 0.2 x 0.1	0.4 x 0.2 x 0.1	0.5 x 0.2 x 0.04	0.3 x 0.2 x 0.05	0.7 x 0.1 x 0.1
Crystal system	Monoclinic	Orthorhombic	Triclinic	Monoclinic	Triclinic	Monoclinic	Triclinic	Monoclinic
Space group	P2 ₁ /c	Pbca	P-1	P2 ₁ /c	P-1	P2 ₁ /c	P-1	P2 ₁ /c
Unit cell dimensions								
<i>a</i> [Å]	7.1350(5)	26.7188(12)	9.2045(7)	12.2051(7)	8.2022(7)	11.642(2)	9.9857(7)	21.3116(15)
<i>b</i> [Å]	13.4037(10)	15.3519(4)	9.6554(7)	8.2650(4)	10.4067(6)	34.953(3)	10.9449(9)	7.3046(4)
<i>c</i> [Å]	19.1020(19)	30.0067(10)	10.2207(6)	20.3470(12)	12.5188(8)	12.436(2)	16.9919(12)	15.4703(11)
<i>α</i> [°]			85.372(5)		94.473(5)		88.604(6)	
<i>β</i> [°]	100.644(8)	90	82.703(5)	97.161(5)	106.385(7)	115.24(2)	83.954(6)	104.104(7)
<i>γ</i> [°]			77.930(7)		106.534(6)		73.579(7)	
<i>V</i> [Å ³]	1795.4(3)	12308.3(8)	879.70(11)	2036.5(2)	968.13(13)	4577.2(15)	1771.4(2)	2335.7(3)
<i>Z</i>	4	16	2	4	2	4	2	4
<i>D</i> _{calc} (g cm ⁻³)	1.339	1.350	1.404	1.409	1.482	1.418	1.347	1.388
No. measd. refl.	13647	38167	7736	9018	6215	17990	13389	9914
no. unique refl. (<i>R</i> _{int})	4373 (4.2%)	14511 (5.5%)	4046 (2.8%)	4679 (2.3%)	3530 (1.9%)	8354 (9.3%)	6449 (8.8%)	5438 (0.0488)
No. obs. refl.	2463	5731	3252	3117	2745	3462	1828	2765
<i>Final R</i> ₁ , <i>wR</i> ₂ (obs. refl.)	5.3%, 11.9%	6.6%, 19.9%	4.6%, 11.9%	4.8%, 12.1%	4.1%, 10.3%	7.2%, 12.9%	6.5%, 9.7%	5.9%, 14.1%
Goodness-of-fit (obs. refl.)	0.969	0.807	0.857	0.884	0.959	0.974	0.830	0.903

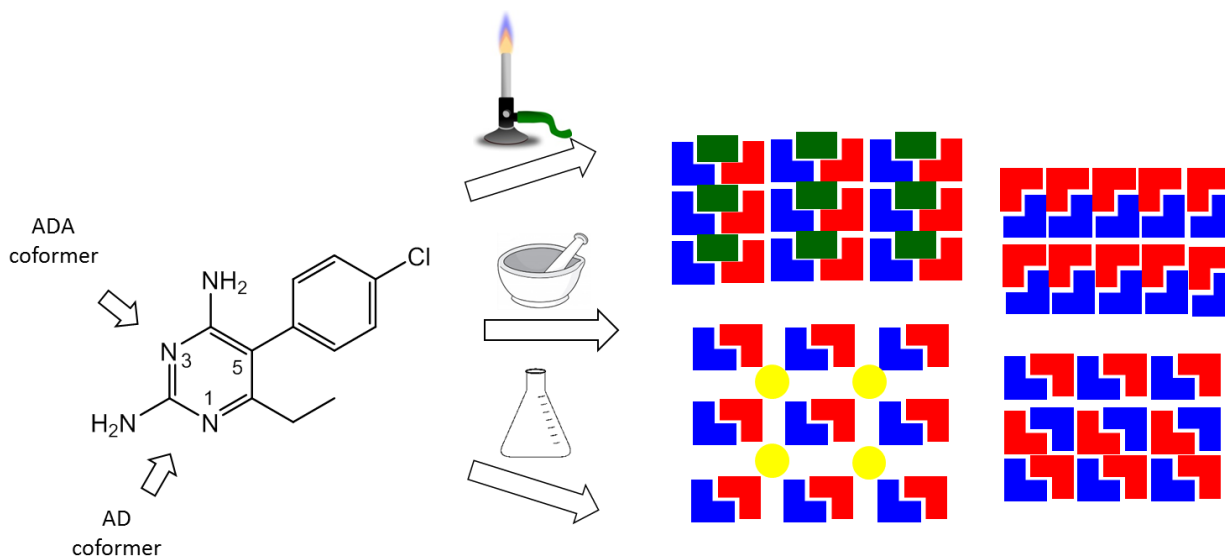
Table 2. Comparison of sublimation, solution crystallization and liquid-assisted milling as methods for the preparation of cocrystals.

	solution crystallization	sublimation	milling
preparation time	several days	< 1 d	< 1 h
scale	easy scale-up	50 – 100 mg	0.1 – 1 g
yield	high; depends on system	tunable to be quantitative	usually quantitative
purity	depends on system	high	usually high
X-ray suitable	yes	yes	no
single crystals			
advantages	easy scale-up	high quality single crystals; solvent-free; independent on solubility	solvent-free or catalytic amounts of solvent; independent on solubility
disadvantages	risk of formation of solvates; solubility issues; can involve excessive volumes of solvents during screening	limited to thermally stable and sublimable cofomers	no single crystals

For Table of Contents Use Only

Salts, Binary and Ternary Cocrystals of Pyrimethamine: Mechanosynthesis, Solution Crystallization and Crystallization from the Gas Phase

Ciaran O'Malley, Chloe Bouchet, Grayce Manyara, Patrick McArdle, and Andrea Erxleben



SYNOPSIS

15 new binary and ternary cocrystals and cocrystal salts of the antimalaria drug pyrimethamine including polymorphs and pseudopolymorphs were obtained by co-sublimation, solution crystallization and liquid-assisted grinding.